IQALUIT CALIBRATION/VALIDATION SUPERSITE FOR METEOROLOGICAL SATELLITES

Z. Mariani[1], A. Dehghan[1], G. Gascon[2], P. Joe[1], K. Strawbridge[3], W. Burrows[1], S. Melo[1]

[1]Cloud Physics and Severe Weather Research Section, [2]Meteorological Service of Canada Prediction and Services, [3]Air Quality Processes Research Section: Environment and Climate Change Canada, Government of Canada; 4905 Dufferin St., Toronto, ON, CAN; M3H-5T4.

E-mail: zen.mariani@canada.ca, armin.dehghan@canada.ca, gabrielle.gascon@canada.ca, paul.joe@canada.ca, kevin.strawbridge@canada.ca, william.burrows@canada.ca, stella.melo@canada.ca

ABSTRACT

It is foreseen that the changing climate in the Arctic will result in increased activities, such as marine navigation, resource exploitation, aviation, fishing, and recreation, requiring reliable and relevant weather information. However, processes governing weather systems in the Arctic are not well understood. There is a recognized lack of meteorological observations to characterize the atmosphere and the cryosphere for operational forecasting and to support process studies, satellite and model calibration/validation (cal/val), and for verification. Environment and Climate Change Canada (ECCC) is enhancing the observing capacity of selected sites, including Iqaluit (64°N, 69°W), which is uniquely situated in close proximity to frequent overpasses by polar-orbiting satellites such as ADM-Aeolus, A-Train, GPM, and EarthCARE. Iqaluit's suite of instruments will provide near-real time observations of altitude resolved wind speed and direction, aerosol size and shape, cloud intensity and height, sensible heat flux, turbulence, fog, and precipitation amount/type. Initial results demonstrate their ability to detect fog, blowing snow and very light precipitation (diamond dust).

1. INTRODUCTION

Studies have shown that the changing climate, which is amplified in the Arctic region, induces changes in weather events with a high socio-economic impact [1]. 90% of major global disasters in the past 20 years have been caused by severe weather-related events. An average of 335 weather-related disasters per year were recorded between 2005 and 2014, almost twice the level as during 1985-1994 [2]. As the climate continues to change, information on the weather and climate will become critical in ensuring the health and safety of local communities.

Economic activity in the Arctic is growing due to increasing population, transportation, and resource development with the opening of the North-west passage; therefore the need for reliable and relevant weather information is a pressing issue. However, numerical weather prediction (NWP) models exhibit poor performance >60° N with significant errors in forecasted pressure and winds [3, 4, 5]. The primary cause of these errors is the large geographic gaps in meteorological measurements. However, a cost-effective solution for an observing system which can meet the challenge of providing relevant meteorological information can only be achieved by integrating ground-based, air-based (e.g., aircraft data), and satellite data.

Environment and Climate Change Canada's (ECCC) Canadian Arctic Weather Science (CAWS) sites are designed to address this gap by testing technologies which can provide near-real time meteorological measurements. The goal is to advise on an operational integrated observing system concept that also addresses the needs of local communities. Vertically-resolved wind, temperature, and humidity observations and characterization of fog and light precipitation using active technologies are the primary focus, given the current and future hazardous weather.

The meteorological observations conducted at each site, particularly the Iqaluit supersite, will enable ground-based cal/val of meteorological satellites, such as the ADM-Aeolus, A-Train, GPM, and the future EarthCARE satellite missions. This paper will provide an overview of

Proc. 'Living Planet Symposium 2016', Prague, Czech Republic, 9–13 May 2016 (ESA SP-740, August 2016)

the CAWS sites (current and future) with a particular focus on the existing Iqaluit supersite's instrumentation and measurement capabilities that began in 2015. Initial results will demonstrate the applicability of integrated products.

2. THE CANADIAN ARCTIC WEATHER SCIENCE SITES

Four sites across Canada's Arctic and sub-Arctic regions (Iqaluit, Inuvik, Whitehorse, and the Squamish area) are being equipped with new meteorological instruments to complement existing operational and research surface-based meteorological observations. These sites are shown in Fig. 1. The CAWS site locations were selected to provide increased observational capacity in key points along the primary transportation routes, Arctic storm pathways (Fig. 2), and critical mid-latitude Arctic weather corridors on the west coast of Canada (not shown).

Iqaluit is located above the tree-line and receives some sunlight during wintertime. Commissioning of the Iqaluit site began July 2015. The measurements obtained in Iqaluit are being made available in near-real time to support ECCC Arctic forecast offices in test mode. Inuvik experiences Polar day/night during ~ 3 months of the year while still having enough humidity to sustain exuberant vegetation. Whitehorse and Squamish are located at the mountain ranges on the Canadian west coast in a complex terrain region. These sites will be commissioned in 2016. All instruments are designed to be remotely accessed and require infrequent maintenance. The goal is to generate and demonstrate the application of products from the combination of multiple measurements in near-real time.

Figure 1: CAWS sites for Arctic and sub-Arctic meteorological observations: 1. Iqaluit (Nunavut), 2. Inuvik (North West Territories), 3. Whitehorse (Yukon Territory), 4. Squamish area (British Columbia). Image: © map-of-canada.org

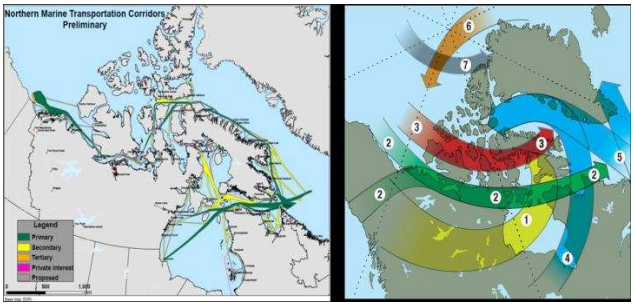

Figure 2: Primary and secondary transport pathways (left) and typical storm tracks (right) in the Arctic region.

3. THE IQALUIT SUPERSITE

Tab. 1 lists the suite of new instruments installed at the Iqaluit supersite in 2015 (in black), together with the suite of instruments which will be installed in 2016 (in green). These measurements complement the existing surface and radiosonde meteorological measurements. This is also an ECCC site for the inter-comparison of solid precipitation gauges and has a Double Fence International Reference. Primarily, these instruments provide year-round automated observations of altitude resolved wind speed & direction, aerosol size and shape, precipitation amount and type, cloud intensity and height, sensible heat flux, turbulence, and water vapour in the atmosphere during different weather conditions including clear skies, fog, blowing snow, and precipitation.

Table 1: Instruments at the Iqaluit supersite, including their deployment date and primary measurement product(s).

Instrument	Manufacturer	Date of Deployment	Operation	Measurement(s)	Temporal/geographic resolution
Ka-Band Radar	METEK	Sept. 2015	Pulsed dual-polarization Doppler Radar	Line-of-sight wind speed and direction, cloud & fog backscatter, depolarization ratio	10 min / 10 m res. up to ~30 km range
Ceilometer	VAISALA	Sept. 2015	Pulsed (8 kHz) diode laser Lidar	Cloud intensity and height, aerosol profiles, PBL height	5 min / 5 m vert res. up to 7.5 km a.g.l.
Radiometer	Radiometrics	Sept. 2015	Profiling microwave radiometer	Profiles of T, RH, dew point T, vapor density	3 min / 10 m vert. res. up to 10 km a.g.l.
PWD 52 Vis. Sensor	VAISALA	Sept. 2015	Forward-scatter measurement	Visibility, precipitation type	1 min / surface obs. only
Doppler Lidar	HALO	Sept. 2015	Pulsed (10 kHz) scanning at 1.5 µm (Mie scattering)	Line-of-sight wind speed and direction, aerosol backscatter, depolarization ratio	5 min / 3 m res. up to ~5 km range
PIP snowflake camera	N/A	Sept. 2015	Automated back-lit camera	Snowflake images	1 min / surface obs. only
Surface met obs.	Misc.	Ongoing	Misc.	Surface T, RH, pressure, winds, precipitation	1 min / surface obs. only
Radiosondes	VAISALA	Ongoing	N/A	Profiles of T, RH, pressure, winds	12 hours / ~15 m res. up to ~30 km a.g.l.
Doppler Lidar (x4)	HALO	Aug. 2016	Pulsed (10 kHz) scanning at 1.5 µm (Mie scattering)	Line-of-sight wind speed and direction, aerosol backscatter, depolarization ratio	5 min / 3 m res. up to ~5 km range
Scintolometer (x2)	Scintec	Aug. 2016	Large-aperture optical transmitter/receiver	Turbulence, crosswind, heat flux	5 min / max 6 km path length
449 MHz Wind Profiler Radar	DeTect	Oct. 2016	Phased-array antenna with full beam steering	3D vertical wind profiles	10 min / 100 m res. up to ~8 km a.g.l.
Aerosol LiDAR	N/A	Aug. 2016	355/532/1064 nm transmitter & 6 ch. receiver	Profiles of aerosols, T, RH, pressure, water vapour, and aerosol size & shape	1 min / 3 m res. up to ~15 km a.g.l.
Multi angle snowflake camera	N/A	Aug. 2016	Automated front-lit high-res. cameras	Snowflake images	1 min / surface obs. only

Commissioning and evaluation of the new instruments at the Iqaluit supersite is currently underway. Instrument survivability and performance during the extreme weather experienced in the Arctic can be considerably different than in southern latitudes. For instance, the Doppler Lidar's measurement range is less in Iqaluit compared to the mid-latitudes. The Lidar's range in Iqaluit is between 1 and 4 km, depending on atmospheric conditions, whereas the same Lidar deployed in the summer of 2015 in Toronto, Ontario, Canada, had a range between 2 and 5 km. The increased range experienced in Toronto can be attributed to the larger number of backscatterers in Toronto's more humid atmosphere compared to that of Iqaluit.

4. IQALUIT SUPERSITE: INITIAL RESULTS

4.1 Surface Wind Maps and Vertical Wind Profiles

A Doppler wind Lidar and Ka-band radar are currently the primary instruments measuring 3-D winds at Iqaluit; they perform automated plan position indicator (PPI; constant elevation scans), range height indicator (RHI; 'over the top' constant azimuth scans North-South and along the 135^{o} azimuth), vertical stare, and wind profile measurements every five and 10 minutes, respectively. No significant downtime was encountered by either instrument throughout the Arctic winter. Both instruments measure the aerosol backscatter intensity, wind speed, and wind direction along their line of sight during different weather conditions (clear-sky, fog, precipitation, etc.). Their scan sequences are fully customizable and can measure in any direction (elevation or azimuth).

Example wind observations made during clear skies on January 19, 2016, from the Doppler Lidar are shown in Fig. 3 (Ka-Radar products are similar). The PPI scan (left) maps surface winds and can be used to estimate the variance in horizontal wind speeds, the wind profile (top-right) provides vertical wind speed and direction up to the planetary boundary layer, and the RHI scan (bottom-right) measures a vertical cross-section of the wind structure. In September 2016 a 449 MHz wind profiler radar system will be installed in Iqaluit to complement these measurements by providing vertical wind profiles (u, v components of the wind field) up to ~ 8 km a.g.l.

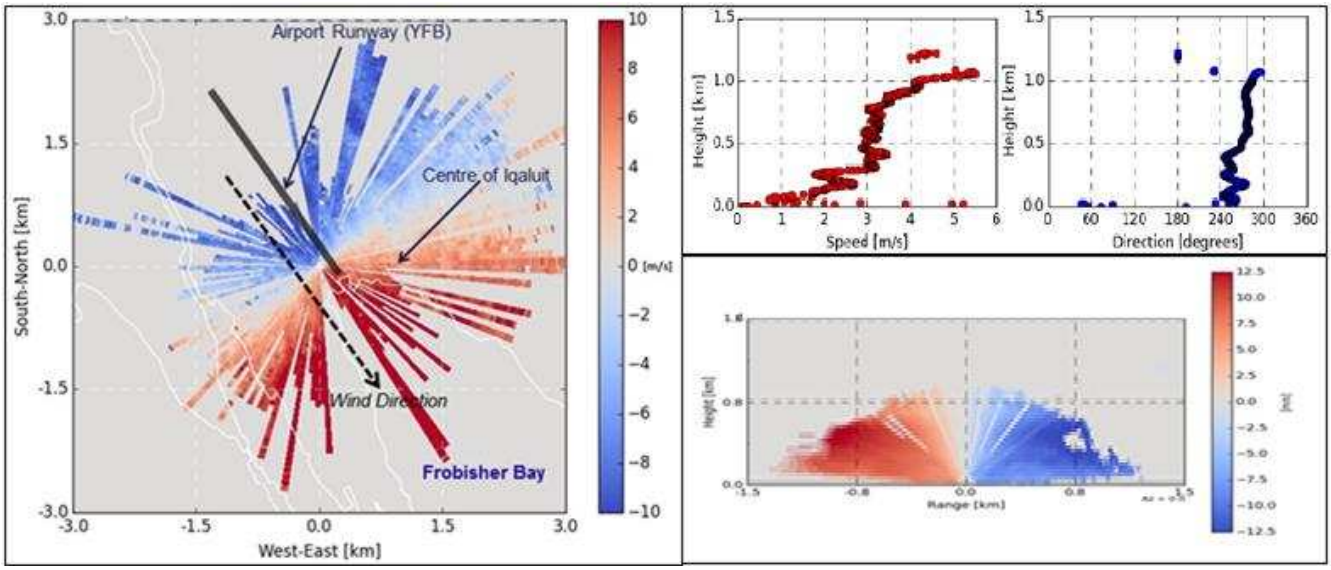

Figure 3: Doppler Lidar measurements of wind speed and direction on April 7, 2016 at 12:39 UTC. Left: PPI surface wind map. Top-right: vertical wind profile up to the planetary boundary layer. Bottom-right: North-South RHI scan of the vertical wind structure. Negative wind speeds (blue) indicate winds towards the Lidar; positive (red) indicate winds away from the Lidar. Similar scans are performed by the Ka-Radar at lower resolution but greater range.

4.2 Observations of Blowing Snow Events

Low-altitude blowing/drifting snow is a common occurrence yet challenging measurement for surface sensors [6]. There is a strong need to separate falling from blowing snow events in order to estimate precipitation amounts and snow movement. Also, precipitation gauges have poor detection capability. The limit of detectability is generally about 0.5 mm/h for the current generation of operational gauges. About 60% of the precipitation in the Arctic is reported as "trace" and not detected. In addition, wind affects the snow gauges – an unshielded gauge will measure only about 20% of the precipitation (> 0.5 mm/h) at 8 m/s [7, 8]. Blowing snow events can cause a significant decrease in visibility that affects the safety of local communities and air- and sea-transportation, and complicate satellite ground-return measurements. The active instruments (Lidar, ceilometer, radar) installed at Iqaluit can detect blowing snow, measuring the evolution and properties of a blowing snow layer's height, thickness, visibility, wind speed and wind direction.

Example observations of blowing snow from the ceilometer, radiometer, and Ka-Radar are shown in Fig. 4, 5, and 6, respectively. A blowing snow layer was visually observed and detected by the ceilometer, extending from the surface up to 400 m on March 14-15, 2016 (Fig. 4). Periods of intensive blowing snow on January 19, 2016 coincided with an increase in surface wind speeds (> 12 m/s) and increases in relative humidity near the surface detected by the radiometer (Fig. 5). A Ka-Radar PPI scan of the blowing snow's backscatter return signal on January 19, 2016 (Fig. 6) measured its horizontal extent. Blowing snow events correlated with a significant decrease in surface visibility measured by the PWD52 visibility sensor and METAR/TAF report issued by NavCanada at the Iqaluit YFB airport (not shown).

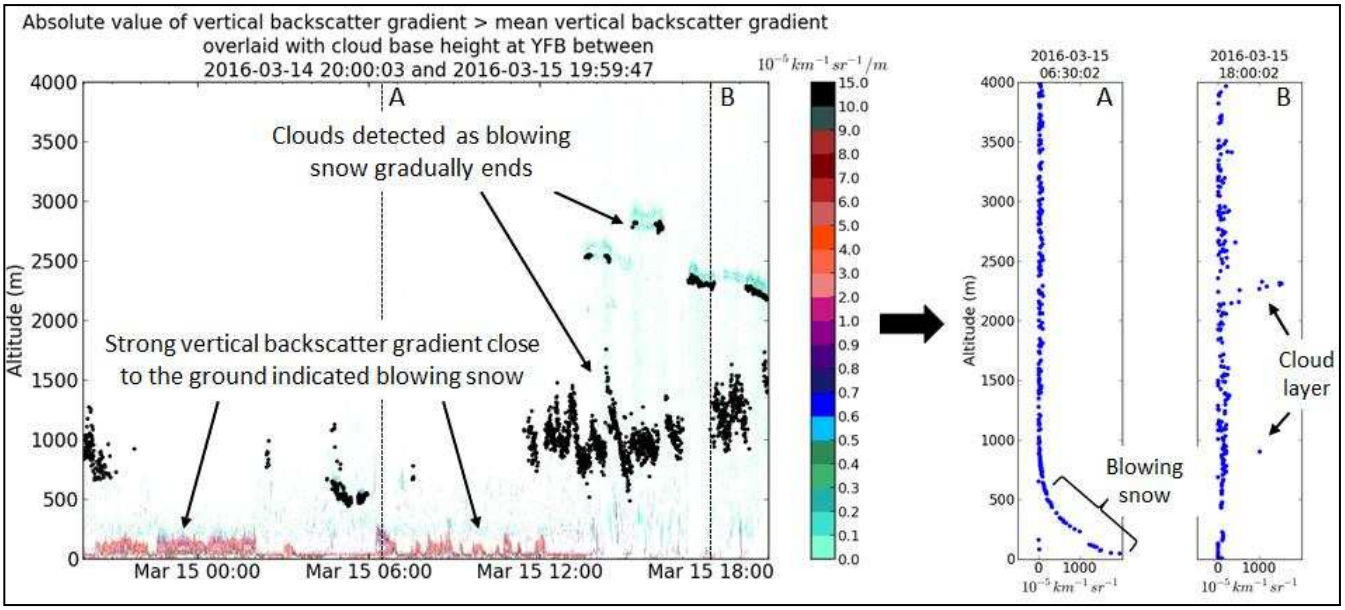

Figure 4: Ceilometer post-processed vertical backscatter and cloud detection (left) and backscatter profiles (right) during a blowing snow event (A) and clouds (B) at Iqaluit on March 14-15, 2016.

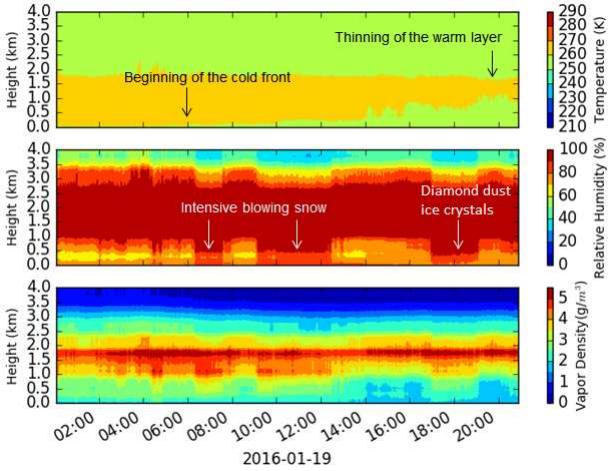

Figure 5: Radiometer temperature (top), relative humidity (middle), and vapour density (bottom) profiles during the blowing snow event on January 19, 2016. Increases in low-altitude relative humidity occurred during times of intensive blowing snow and diamond dust ice crystals.

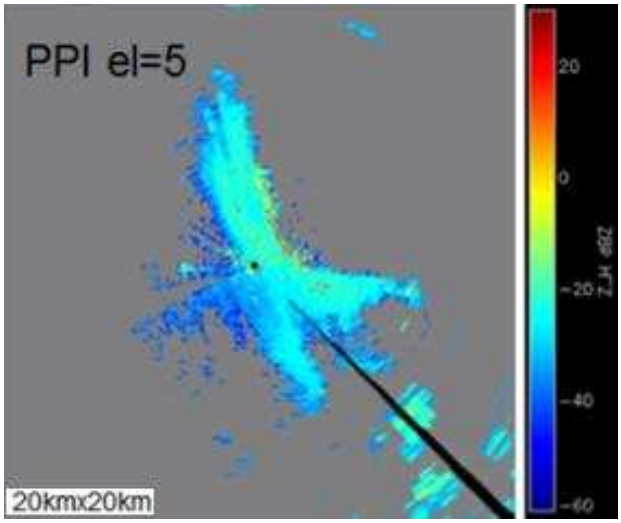

Figure 6: Ka-Radar PPI horizontal scan during the blowing snow event on January 19, 2016 at 22:00 UTC. The observed backscatter signal (-30 to -60 dBZ) mapped the horizontal structure of blowing snow detected near the surface. The PPI scan's elevation was 5°.

4.3 Observations of Diamond Dust Ice Crystals

Ice crystals (also referred to as diamond dust) alter the radiative balance and create a net cooling effect of the atmosphere [9, 10]. Their presence is not detectable using operational precipitation gauges. The ceilometer, Doppler Lidar, Ka-Radar, and optical visibility sensors (not shown) are capable of directly detecting the presence of these small ice particles. On January 20, 2016, an enhancement in the intensity from the ceilometer data and the aerosol backscatter signal from the Lidar was observed between 16:00 to 17:00 UTC (Fig. 7), coinciding with a diamond dust event that was visually observed. Following the diamond dust event, surface winds increased, causing low-level blowing snow up to 300 m a.g.l as was detected by both instruments. Doppler Lidar and Ka-Radar depolarization ratio (ice vs. water classification) measurements indicated the presence of ice crystals throughout the ice crystal layer during this time (not shown) and provide altitude-resolved ice crystal/super-cooled water discrimination

4.4 Measurements of the Planetary Boundary Layer Height

The planetary boundary layer (PBL) height, sometimes referred to as the mixing layer height, is a critical dynamical feature parameterized in NWP models, affecting forecast accuracy [11]. The ceilometer's backscatter gradient measurements provide estimates of the PBL height with high temporal and altitude resolution using edge-detection algorithms. This enables tracking of sudden changes in the PBL height attributed to changes in air mass (Fig. 8). This data, integrated with collocated radiometer, Doppler Lidar, aerosol Lidar, and radar observations provide essential altitude-resolved meteorological parameters required to validate, verify and improve the NWP model in the Arctic.

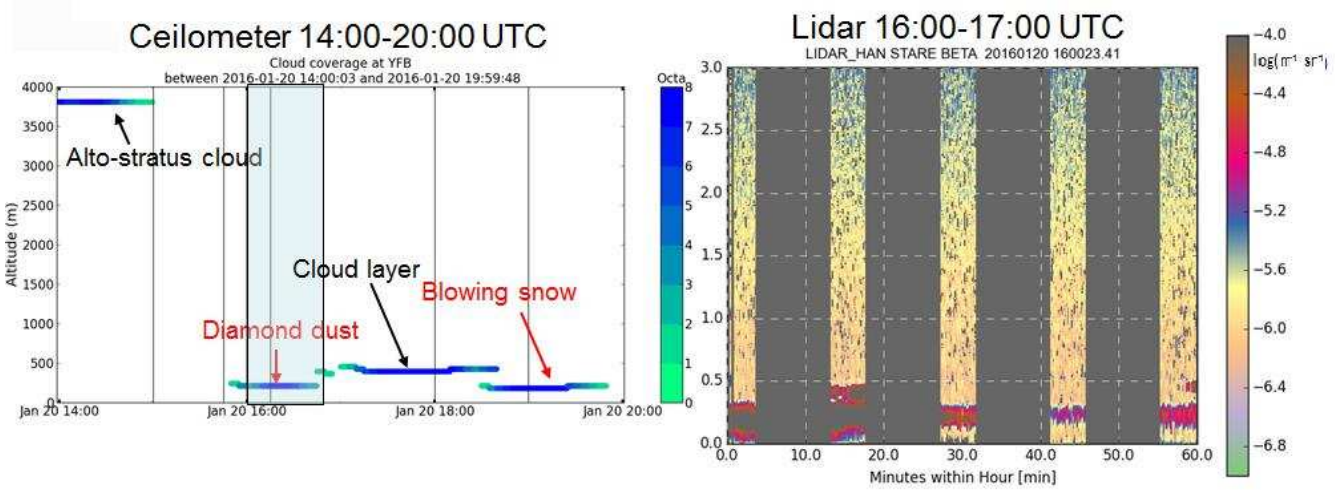

Figure 7: Ceilometer cloud intensity algorithm (left) during varying cloud and light precipitation conditions (labelled). The shaded region corresponds to the time period of the Doppler Lidar measurements shown on the right, also detecting the presence and thickness of ice crystals below 500 m. Grey columns indicate when the Lidar was performing other scans.

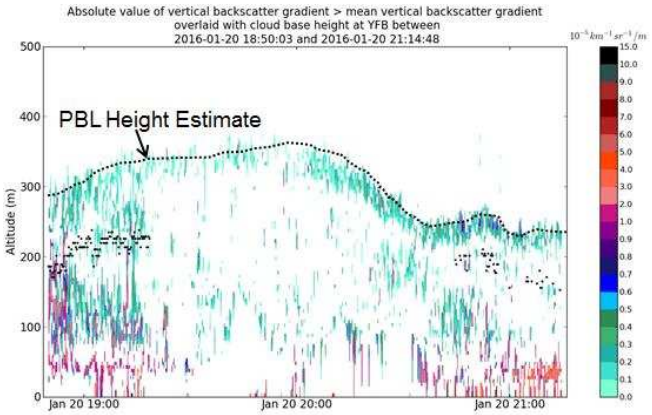

Figure 8: Example ceilometer PBL height estimate (black dotted curve) via vertical backscatter gradient observations on January 20, 2016.

Figure 9: Arctic aerosol/water vapour Lidar to be installed fall 2016.

4.5 Arctic Aerosol/Water Vapour Lidar

The Arctic aerosol/water vapour Lidar [12] (Fig. 9) will be installed at Iqaluit in the fall of 2016. It will conduct automated continuous measurements (except during precipitation) of the vertical structure of particulate matter up to 15 km a.g.l. The Lidar has recently been upgraded with a new Licel data acquisition system and Northrop Grumman Gigashot three wavelength solid state diode laser and six-channel receiver, enabling: 1) simultaneous measurements of aerosol profiles at all wavelengths including particle size and shape, 2) depolarization ratio measurements at 355 nm, and 3) night time water vapour measurements using a Raman technique.

5. CONCLUSIONS

Four ECCC sites are being equipped with new meteorological instruments based on active technologies as part of the CAWS Project to enhance existing surface meteorological observations. These sites will provide near-real time data aimed to improve weather forecasts in the Arctic. The sites have been designed to support ground-based cal/val of meteorological satellites, such as ADM-Aeolus, A-Train, GPM, and EarthCARE. A microphysics aircraft campaign is also being planned in the Arctic in conjunction with the WMO Year of Polar Prediction Project (2017). In particular, this contribution focussed on the commissioned Iqaluit supersite.

Observations at these sites are made to provide: (1) detailed, high temporal-resolution profiles of wind, temperature, humidity, cloud microphysics, and aerosol measurements, (2) horizontal and in some cases 3-D mapping of these variables, allowing retrieval, variability, and satellite uncertainty studies, (3) complementary analysis of ground-return signal over Arctic terrain, (4) coordinated pan-Arctic sites, (5) aircraft cal/val field campaign studies, and (6) long-term satellite measurement cal/val.

Initial results at the Iqaluit supersite indicate its unique ability to provide reliable, relevant, and continuous meteorological measurements of the horizontal and

vertical structure of winds, aerosol size and shape, precipitation amount and type, cloud intensity and height, surface visibility, profiles of air and dew point temperature, relative humidity, vapour density, sensible heat flux, and particle type during different weather conditions at high temporal resolution (<10 minutes). In particular, the ability to detect and measure the thickness, height, and composition of blowing snow and diamond dust ice crystals has been demonstrated. The Iqaluit supersite, along with the other CAWS sites, are expected to be fully-equipped and delivering data products in test mode, on a continuous, automated basis, by fall 2016.

6. REFERENCES

[1] WMO (2011): Weather extremes in a changing climate: hindsight on foresight. *World Meteorological Organization (WMO)*; WMO-No. 1075, pp. 1-20.

[2] UNISDR (2015): The human cost of weather-related disasters 1995-2015. *United Nations Office for Disaster Risk Reduction (UNISDR)*; pp. 1-30.

[3] Cassano, J., Higgins, M., and Seefeldt, M. (2011): Performance of the Weather Research and Forecasting Model for Month-Long Pan-Arctic Simulations. *Mon. Wea. Rev.*; 139, 3469–3488.

[4] Schyberg, H. and Randriamampianina, R. (2015): MET Norway plans for contribution to calibration-validation and use of Aeolus winds. *ADM-Aeolus Science and Cal/Val Workshop*; ESRIN, Frascati, 10-13 Feb.

[5] Riishojgaard, L. (2015): Wind Measurements in the WMO Global Observing System. *ADM-Aeolus Science and Cal/Val Workshop*; ESRIN, Frascati, 10-13 Feb.

[6] F. Naaim-Bouvet, H. Bellot, K. Nishimura, C. Genthon, C. Palerme, G. Guyomarc'h, and V. Vionnet (2014): Detection of snowfall occurrence during blowing snow events using photoelectric sensors. *Cold Reg. Sci. and Tech.*; 106-107, 11-21.

[7] Goodison, B.E., Louie, P.Y.T., and Yang, D. (1998): WMO solid precipitation measurement inter-comparison – Final report. *World Meteorological Organization(WMO)*; Instruments and observing methods Report No. 67, WMO/TD No. 872.

[8] Rasmussen, R., Baker, B., Kochendorfer, J., Meyers, T., Landolt, S., Fischer, A., Black, J., Thériault, J., Kucera, P., Gochis, D., Smith, C., Nitu, R., Hall, M., Ikeda, K., and Gutmann, E. (2012): How Well Are We Measuring Snow? The NOAA/FAA/NCAR Winter Precipitation Test Bed. *Bull. Amer. Meteor. Soc.;* 93, 811-829, doi: http://dx.doi.org/10.1175/BAMS-D-11-00052.1.

[9] Y. Gotaas and C. S. Benson (1965): The Effect of Suspended Ice Crystals on Radiative Cooling. *J. Appl. Met.*; 4, 446–453, doi: 10.1175/1520-0450/1965/004/0446:TEOSIC.

[10] Lebo, Z. J., N. C. Johnson, and J. Y. Harrington (2008): Radiative influences on ice crystal and droplet growth within mixed-phase stratus clouds. *J. Geophys. Res.*; 113, D09203, doi:10.1029/2007JD009262.

[11] Vogelezang, D. H. P., and A. A. M. Holtslag (1996): Evaluation and model impacts of alternative boundary-layer height formulations. *Bound.-Layer Meteor.*; 81, 245-269, doi:10.1007/BF02430331.

[12] Strawbridge, K. (2013): Developing a portable, autonomous aerosol backscatter lidar for network or remote operations. *Atmos. Meas. Tech.*; 6, 801-816, doi: 10.5194/amt-6-801-2013.